Solvent-Induced Stereochemical Behavior of a Bile Acid-Based Biphenyl Phosphite: A Computational Study†

Antonella Cimoli, Giacomo Prampolini, and Alessandro Tani*

Dipartimento di Chimica e Chimica Industriale, Università di Pisa, via Risorgimento 35, I-56126 Pisa, Italy

Received: May 29, 2009; Revised Manuscript Received: September 8, 2009

The origin of the stereochemical behavior experimentally found in a bile acid-derived biphenyl phosphite is studied by means of quantum mechanical methods. The molecular mechanisms driving the screw sense of the dihedral angle between the two phenyl rings of the biphenyl phosphite unit are investigated with density functional theory calculations. Energy, geometry, and circular dichroism spectra have been computed and compared between the two resulting diastereoisomers. We evaluated the solvent effect on the torsional energy profile by discussing the results obtained for the isolated molecule with those found with polarizable continuum model (PCM) calculations performed in different solvents. The results we obtain with the PCM model do not reproduce the solvent effect on the stereochemical equilibrium of this phosphite.

1. Introduction

There is a large and growing interest for restricting and, even more, controlling mechanical motions at the molecular level.[1] Among the mechanisms that control unidirectional motion are redox events[2] and photochemical isomerizations.[3] For instance, the latter mechanisms can lead to quite remarkable effects when the molecule that undergoes photochemical isomerization is used as a dopant in liquid crystals (LCs). Azobenzenes are the most largely studied example, and their ability to change shape upon irradiation allows for the modulation of many LC properties, such as transition temperatures, helical twisting power, and spontaneous polarization,[4] providing the basis for photonic applications.[5] Photochemical isomerization is an example of a well-understood mechanism for controlling molecular motion. In other cases, unidirectional bond rotation is achieved by combined steric restrictions and dipole−dipole interactions, for example, in atropoisomeric amides[6] and 2-aryl-pyridines.[7] However, controlling molecular motion is, in general, a very challenging task, so understanding the mechanism of spontaneous unidirectional motion can provide valuable clues for a more effective design of molecular devices.

An interesting example of solvent control over a torsional motion has recently been[8] observed for a biphenyl phosphite molecule, hereafter referred to as BADBP (methyl 3α-acetyloxy-12α-(biphenyl-2-2′-diyl)phosphite-5β-cholan-24-oate). (See Figure 1.) In the same work, other derivatives where the phosphite has been moved to position three or seven have also been studied. The stereochemically different environments they produce lead to different behavior of the torsional motion around the ring−ring bond of the biphenyl (BP) unit. Cotton effects, revealed by circular dichroism (CD) spectra, are present in the region 230−300 nm only if the BP group is twisted in a prevalent screw sense. Cotton effects of opposite sign are observed when the CD spectra of the compound with linking position 12 or 7 are recorded. No band is visible in the region 230−300 when the BP moiety is linked to position three.

The most relevant finding is that BADPB with biphenyl phosphite in position 12 (and not the others) shows different CD spectra according to the solvent. In particular, the CD spectrum in acetonitrile (ACN) is in an enantiomeric relationship with the one obtained in tetrahydrofuran (THF). Because the sign of the Cotton effect depends on the prevalent screw sense of the BP chromophore, this means that the solvent itself induces a particular negative (M) or positive (P) torsion: the equilibrium between the two diastereomers is shifted toward the M or P form, respectively, in ACN or THF. This is definitely an intriguing result and would mean that by using BADBP as a chiral inducer in particular reactions (where the enantioselectivity depends on the absolute conformation of the BP fragment), different enantiomers of a same product could be obtained simply by changing the solvent.

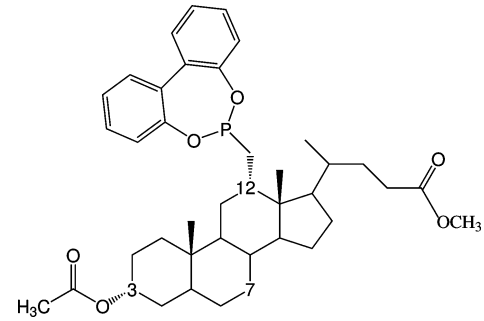

Figure 1. Bile acid-derived biphenyl phosphite (BADBP): methyl 3α-acetyloxy-12α-(biphenyl-2-2′-diyl)phosphite-5β-cholan-24-oate.

A deeper insight into the molecular mechanisms determining the behavior of BADBP conformers can be achieved by facing the problem from a computational point of view. First of all, reliable[9] CD spectra can be computed through time-dependent density functional theory (TDDFT) and compared with their experimental counterparts, thus allowing us to assess a correspondence between the sign of the Cotton effect and the screw sense of the BP group. More important, by comparing results for the isolated and solvated molecule, it is possible to understand if the origin of the investigated mechanism is purely induced by the solvent or some kind of intramolecular interaction should be taken into account.

This article is organized as follows: Section 2 contains the computational details of the performed density functional theory

† Part of the "Vincenzo Aquilanti Festschrift".

* Corresponding author. E-mail: tani@dcci.unipi.it.

10.1021/jp905062q
Published on Web 10/09/2009

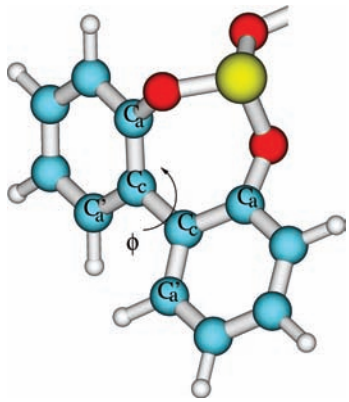

Figure 2. Definition of the torsional angle, ϕ, in the biphenyl fragment. During optimizations the torsional angle has been fixed by constraining the two dihedral angles $<C_aC_cC_cC_a$ and $<C'_aC_cCcC'_a$ to the chosen ϕ value. This definition of ϕ was adopted for all molecules investigated, namely, BADBP, methyl−biphenyl phosphite, and biphenyl.

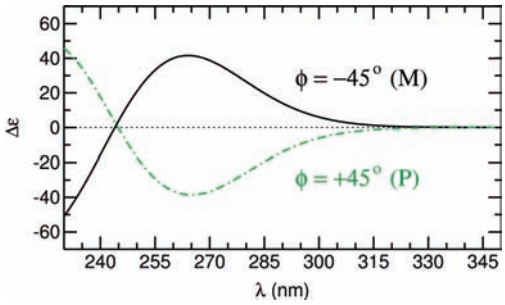

Figure 3. TDDFT-computed CD spectra of methyl−biphenyl phosphite. Calculations were performed on the isolated molecule with the B3LYP density functional and the cc-pvdz basis set.

(DFT) calculations, whose results are reported in Section 3, whereas main conclusions are collected in the last section.

2. Computational Details

All calculations were performed with the GAUSSIAN 03 package,[10] making use of the well-tested density functional B3LYP[11] with a correlation-consistent basis set, cc-pvdz. In the calculation of electronic CD spectra, TDDFT was employed with the lowest-energy 30 exited states, as suggested in ref 8.

The torsional potential energy curve was computed at a DFT level on the isolated molecule by optimizing all geometries with no symmetry restrictions but the investigated torsional angle, ϕ, whose definition is sketched in Figure 2. Because in all cases both aromatic rings remain practically planar, ϕ can be defined as the dihedral angle between the two phenyl rings. The absolute energy minimum was obtained by a complete geometry optimization.

To take into account the solvent effect, we computed the same potential energy curve by using the polarizable continuum method (PCM[12]) in the polarizable conductor calculation model (CPCM[13,14]) using ACN and THF. Both solvents were described by standard parameters, that is, a dielectric constant of $\varepsilon = 36.64$ and 7.58 and a radius of 2.155 and 2.56 Å, for ACN and THF, respectively. Unless otherwise stated, CPCM calculations were undertaken on the geometries previously relaxed in vacuum without performing any further optimization. The cavity that contains the solute is described in the "solvent excluding surface" (SES) convention, whereby the surface is generated by the atomic or group spheres and by the spheres created automatically to smooth the surface.

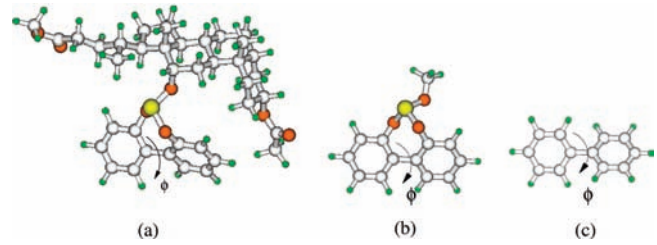

Figure 4. Investigated molecules: (a) deoxocholic acid-derived phosphite (BADBP); (b) methyl−biphenyl phosphite (MBP); (c) biphenyl (BP).

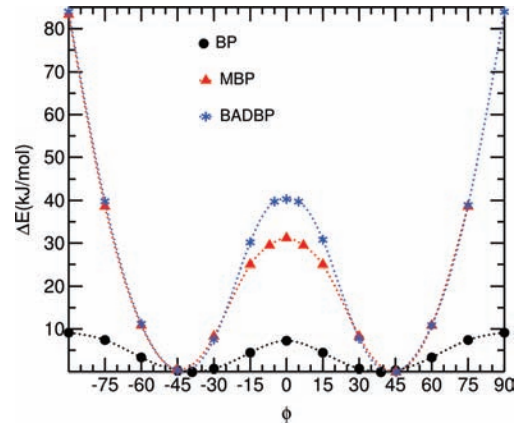

Figure 5. Comparison of torsional energy curves of BADBP (blue stars) with that of MBP (red triangles) and BP (black dots). All data are from DFT calculations.

3. Results and Discussion

3.1. Isolated Molecule. The experimental Cotton effect, found[8] in the 230−300 nm range for the BADBP molecule, was attributed to a prevalent screw sense in the twist of the BP group because the only electrical dipole-allowed transitions optically active in that wavelength region are those of the BP chromophore. Moreover, the sign of this Cotton effect depends on that of the ϕ dihedral, a key feature of the problem. The conformation of BADBP, which originates the positive (negative) Cotton effect, can be deduced, making a comparison between the experimental CD solvent spectra and the theoretical one of a model compound in a known conformation.[8] The CD spectra were computed for M ($\phi = -45°$) and P ($\phi = +45°$) conformations of the methyl−biphenyl phosphite (MBP) molecule, with a larger basis set then that used in ref 8. Our results, reported in Figure 3, confirm the findings of ref 8, namely, that a negative Cotton effect results when MBP is in P conformation, whereas a positive band turns up when the M conformer is investigated. Because experimental BADBP's CD spectra in ACN and THF have positive and negative bands, respectively, the two conformers are assigned $\phi = -45°$ (M) conformation in the first case and $\phi = +45°$ (P) in the second solvent.

Given the large molecular dimensions of the BADBP molecule, it would be desirable to perform most of the quantum mechanical calculations on a smaller molecular model that retains all of the features that determine the behavior of the investigated torsion. With this aim, the torsional energy profiles of MBP and BP molecules (Figure 4) were computed and compared with the curve obtained for the parent BADBP compound. The results are reported in Figure 5.

The BP torsional potential has been extensively studied with many quantum mechanical approaches,[15,16,18,19] and the present combination of method/basis set shows good agreement with literature results, thus validating the reliability of this choice.

In particular, the BP torsional curve is symmetrical with respect to 0 and 90°, the minimum conformation is found at $\phi \approx \pm 45°$, and the barrier at 0° is ~7 kJ/mol, whereas that at 90° is between 9 and 10 kJ/mol. These features have been explained[18,19] as a consequence of an energetic balance between the conjugation effects of the aromatic rings (which are maximized in a planar conformation and vanish at $\phi = 90°$) and steric repulsion between hydrogens bonded to ortho carbons (which is negligible when the phenyl planes are perpendicular but disfavors the planar $\phi = 0°$ conformation.)

The torsional potential for the two phosphite compounds, MBP and BADBP, changes radically with respect to BP. This is due to the presence of the phosphite group, which is bonded to the ortho carbons of the BP moiety through the oxygen atoms and forms a seven-atom ring. (See Figure 2.) This ring hinders the torsion of the two phenyls around the C−C bond because ϕ values beyond ±90° lead to an unphysical stretching of the P−O and O−C bonds. By looking at Figure 5, it appears that the BADBP barrier at 0° goes up to 40 kJ/mol (four times the BP barrier) and the O−P−O bridge hardens the internal flexibility to such an extent that no rotation can occur beyond ±90° because the O−C and O−P involved bonds would eventually break, as shown by the increasing energy values. The two minima at ±45° remain unshifted with respect to BP and are isoenergetic, maintaining the symmetry of the potential function.

The torsional curve of the smaller MBP molecule is also reported in Figure 5. The comparison between the BADBP and MBP curves can give some information on the role of the cholestanic moiety on the investigated torsion, that is, which effects and features may be ascribed to the cholestanic backbone and which, instead, simply depend on the presence of the phosphite group. The MBP profile is qualitatively similar to that of BADBP: barrier at 0°, isoenergetic minima at ±45°, and energy increase toward ±90°. The main difference is the height of the energy barrier, which is slightly less in the smaller molecule.

BADBP and MBP minima positions are unshifted with respect to BP because 45° is still the best compromise among different effects: the $\pi-\pi$ interaction that would favor a planar geometry, the steric repulsion of the two oxygens that would push toward a $\phi = 180°$ conformation, and the ring with the phosphorus that hinders torsions beyond 90°. It is worth emphasizing the importance of the potential symmetry. There was no reason to expect something different as far as the MBP molecule is concerned, but, on the other hand, the shape of the BADBP torsional potential was not foreseeable: the effect of the cholestanic backbone on the torsional symmetry was not obvious. Because the MBP energy profile maintains almost the same profile as that shown by BADBP, it can be assumed that the cholestanic backbone does not affect the flexibility of the investigated inter-ring dihedral through any intramolecular mechanism.

The flexibility of the ϕ dihedral describing the torsion around the C_c-C_c bond is intrinsically connected to the cyclic structure comprising the seven-atom ring. To further investigate the geometrical transformations occurring to this ring during ϕ torsion, the dependence of some internal coordinates on the torsion angle has been reported in Figure 6. Among these, dihedrals δ_1 and δ_2 describe the torsion around the C_O-O_p and O_p-P bonds, respectively, whereas $\delta_3-\delta_6$ angles drive the seven-atom ring flexibility.

The δ_1 value, which is shown in the top panel of Figure 6, is constant during the ϕ scan, meaning that this internal coordinate

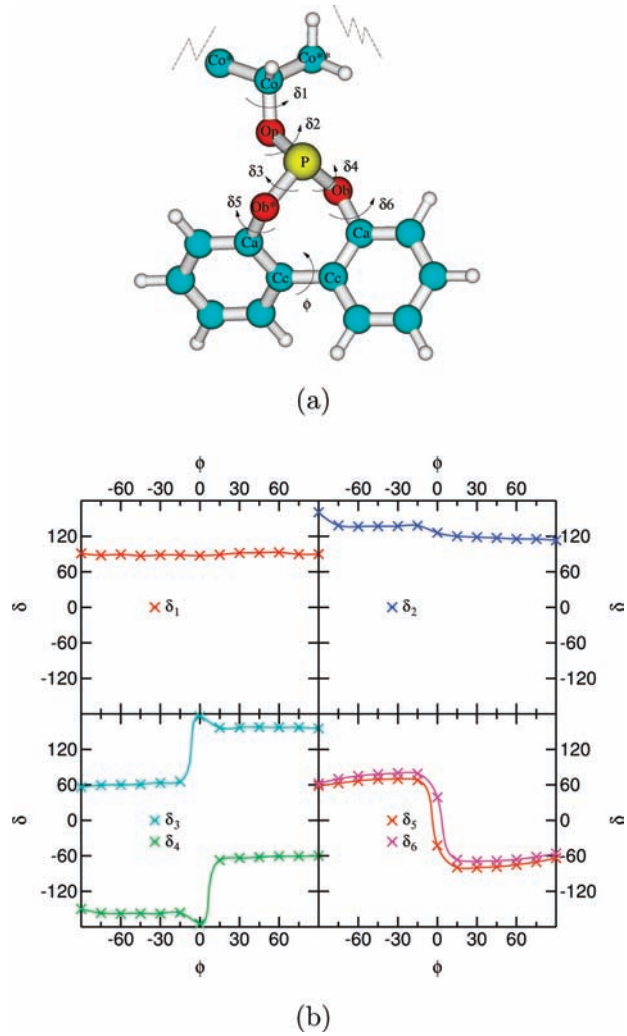

Figure 6. Top panel: sketch of a BADBP fragment with the definition of dihedrals δ_1 to δ_6: only relevant atoms have been drawn and labeled, all the other have been cut away by the zigzag segments. δ_1 and δ_2 have been defined as $C_O^{**}\widehat{C_oO_pP}$ and $C_O\widehat{O_pPO_b^*}$ dihedral angles, respectively. Bottom panel: trends of some BADBP's δ dihedral angles toward a ϕ scan.

is not coupled to ϕ. Also, δ_2 appears essentially uncoupled to ϕ: it undergoes a rather small change (~15°) when ϕ switches from negative to positive values. Because δ_1 and δ_2 are the dihedral angles mostly responsible for the position and orientation of the BP appendage with respect to the cholestanic backbone, the lack of coupling with ϕ confirms the hypothesis that the biliar substrate does not affect the internal BP rotation.

Conversely, there is an apparent coupling with ϕ torsion of the dihedrals $\delta_3-\delta_6$. The first two, respectively, defined as $O_p\widehat{PO_b^*C_a}$ and $O_p\widehat{PO_bC_a}$ (δ_4), correspond to torsions around the $P-O_{b(*)}$ bonds. They both show a strong discontinuity in the nearby barrier region, where they exchange their values ($\phi < 0$: $\delta_3 \simeq 60°$, $\delta_4 \simeq -150°$; $\phi > 0$: $\delta_3 \simeq 150°$, $\delta_4 \simeq -60°$). Finally, δ_5 (ruling the $O_b^*-C_a$ torsion), shows a similar behavior to δ_6 (ruling the O_b-C_a torsion): they have roughly constant values beyond ±15° and an inversion in between (from ~60° to ~−60°).

The behavior of these dihedrals suggests a sort of "switch effect", which takes place when ϕ undergoes a transition from positive to negative values, passing through the highly stretched $\phi = 0$ conformation. A deeper insight into this effect can be gained by looking at Figure 7, where the MBP molecule is seen

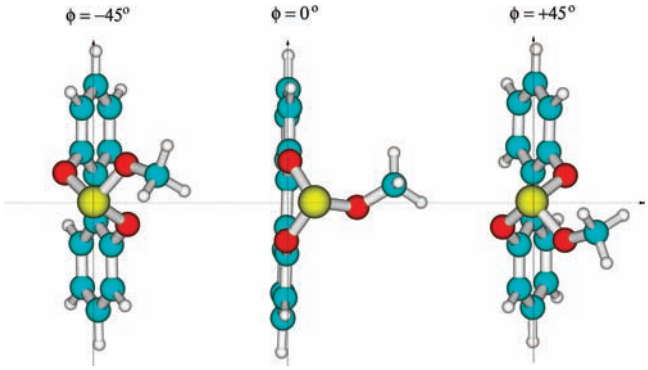

Figure 7. DFT-constrained optimized geometries. From left to right: $\phi = -45$, 0°, and +45° geometries. Horizontal and vertical lines are simply drawn as a guide for the eye.

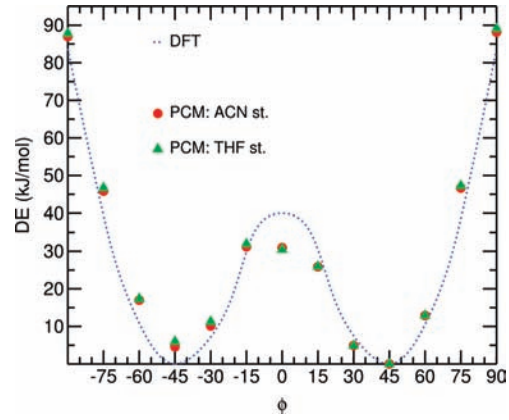

Figure 8. PCM single-point energy curves in ACN and THF for BADBP.

from a point of view on top of the phosphorus atom, highlighting the relative position of the O−P−O bridge segment, the underlying BP edge, and the angle in between, for $\phi = -45$, 0, and +45, respectively. In all $\phi < 0$ optimized geometries, the O−P−O segment is rotated counterclockwise with respect to the BP edge (vertical solid line), whereas the opposite stands for $\phi > 0$ geometries. At $\phi = 0$, instead, the oxygens overlap the BP edge. During this conformational switch, that is, passing from the M ($\phi = -45°$) conformer to the P ($\phi = +45°$) conformer, the oxygens exchange their positions with respect to the vertical line but remain one above and one below the horizontal line. This movement involves all of the δ_3−δ_6 dihedral angles and alters their values to a large extent, as indicated in Figure 6.

In summary, this analysis again suggests a strong coupling, in the MBP molecule, between the phosphorus ring dihedrals and the BP torsion, which determines the Cotton effect observed in CD spectra. Furthermore, the aforementioned mechanisms, which underlie the M−P interconversion, were shown to preserve a high degree of symmetry, which is in agreement with the resulting degeneracy of the two minima. This picture is unchanged when the cholestanic moiety is introduced because the M−P conformations remain isoenergetic and the δ_1, δ_2 dihedral are not affected by the value of the ϕ angle.

3.2. Condensed Phase. The data presented above suggest that the different populations of the two conformers, which causes the Cotton effects experimentally found in the CD spectra, should originate from intermolecular interactions with the solvent rather than some intramolecular mechanism taking place between the chromophore and the cholestanic backbone.

These solute−solvent interactions could be of either electrostatic continuum nature or excluded volume effects or a combination of the two.

In the first case, a continuum description of the solvent, as that provided by the PCM approach, should suffice to give a rationale of the effect of two solvents with strongly different dielectric permittivity. If steric or cage effects are important in describing the population inversion between M and P conformers, then an explicit solvent description should be adopted.

In the first hypothesis, we've addressed some PCM calculations in ACN and THF, two solvents that experimentally result in enantiomeric CD spectra. Because the cholestanic backbone could play an important role in modulating the continuum interactions of the BP chromophore with the solvent, all PCM calculations have been performed on the whole BADBP molecule.

We performed a first set of calculations by computing the torsional profile of the ϕ dihedral in the two solvents by means of the PCM method.

The resulting curves in ACN and THF solvents are reported in Figure 8, together with the torsional profile previously obtained for the isolated molecule.

The energy curves of the two solvents are very similar because for all ϕ conformations, the PCM energies in ACN almost overlap that in THF. The geometries with negative ϕ (in the range $-60 \leq \phi < 0 \leq -15°$) are higher in energy than that with positive ϕ. In particular, the degeneracy of the two M−P minima found for the isolated molecule is lost, and the P ($\phi = +45°$) conformer results are more stable with respect to the M ($\phi = -45°$) conformer by ∼4.5 and ∼ 6.0 kJ/mol in ACN and THF, respectively. Besides the loss of symmetry, it is worth noticing that the barrier height at $\phi = 0°$ is decreased by ∼10.0 kJ/mol with respect to the gas-phase value by the solvent. The reaction intermediate involved in the P−M interconversion is thus stabilized, making the $\phi = +45° \rightleftharpoons -45°$ geometry change less difficult than that in the gas phase.

Further insight into the M−P different stabilization can be gained by looking at Figure 9, where different contributions to the PCM total energy are reported for both solvents. It can be seen that whereas the repulsion contribution (panel d) is almost constant along the whole ϕ scan, the cavitation and dispersion energies (panels b and c) slightly stabilize $\phi > 0$ geometries with respect to the negative ones in the vicinity of the planar conformation. This is more apparent in Figure 10, where the difference between the energy at a given positive ϕ and that at the same, but negative, ϕ is shown.

The sum of the former contributions thus favors the P isomer with respect to the M isomer by ∼2 kJ/mol in both solvents. In addition, the solute−solvent polarization term (panel a) also favors positive ϕ conformations by ∼1 or 2 kJ/mol in ACN and THF, respectively.

In summary, according to PCM results, the preference for the P conformer (and the lowering of the $\phi = 0°$ barrier) derives from a combination of electrostatical, dispersion, and cavitation effects, with no substantial difference between ACN and THF. On the basis of the previous torsional PCM curves reported in Figure 9, it can be confidently hypothesized that, even solvated, the two absolute minima will retain geometries with $\phi \approx \pm 45°$.

However, to verify the possibility that a geometrical relaxation could alter the relative M−P stability, PCM full optimizations of BADBP in these conformations have been performed in the two solvents, and the results are reported in Tables 1 and 2. Even if the difference is decreased, the P ($\phi = +45°$) conformer

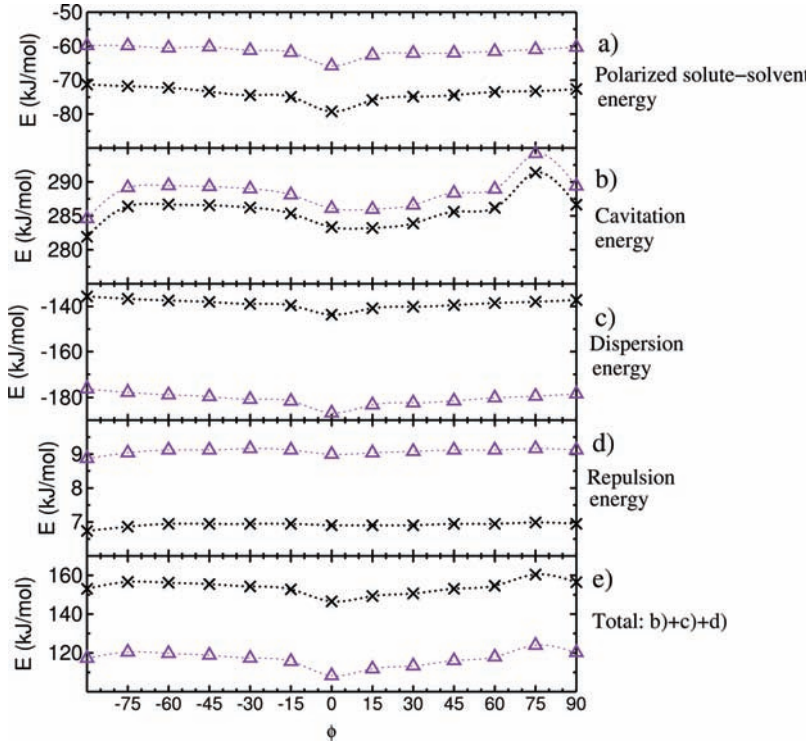

Figure 9. BADBP's PCM energy contributions in ACN (black crosses) and THF (violet triangles). From the top, in the first four panels, the polarized solute−solvent, cavitation, dispersion, and repulsion energies, respectively, are shown. In the bottom panel, the sum of cavitation, dispersion, and repulsion energies is reported.

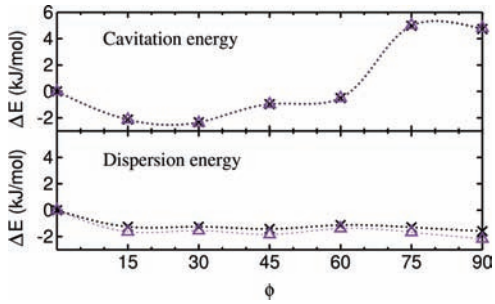

Figure 10. Differences of cavitation and dispersion energies at positive and negative values of ϕ (that is $E(\phi > 0) - E(\phi < 0)$). Data for ACN (black crosses) and THF (violet triangles).

TABLE 1: Energy Difference between the Two Diastereoisomers, Computed by PCM-DFT Calculations in ACN and THF Solvents

	single point		optimization	
	ACN	THF	ACN	THF
$E_M - E_P$ (kJ/mol)	−4.5	−6.0	−3.5	−3.8

is still preferred to the M ($\phi = -45°$) conformer by ∼3.5 and 3.8 kJ/mol, in ACN and THF, respectively. (See Table 1.) In particular, the P absolute energy is very similar to that from the single-point calculation: no significant geometry alterations have occurred during the optimization, as appears from the dihedral values reported in Table 2. The M isomer, on the contrary, decreases its energy more evidently for a total of ∼1 and 2 kJ/mol in ACN and THF.

As far as its geometry is concerned, no great geometrical changes occur in the cholestanic backbone nor in the aromatic rings. However, the relaxation process affects the bond and dihedral angles slightly more than in the case of the P diastereoisomer. More important, the PCM geometry optimizations did not alter the relative position of the two minima in either solvents, confirming the previous conclusions. In fact, our results seem to suggest that the PCM route is unable to account for the population inversion in the two solvents, even if it has been shown to be capable of separating M and P minima. The different cavitation energy contribution for the two isomers may indicate the importance of excluded volume effects, which certainly warrant further investigations.

TABLE 2: PCM Results for the BADBP P ($\phi = +45°$) and M ($\phi = -45°$) Conformers[a]

	P ($\phi = +45°$)			M ($\phi = -45°$)		
		optimization			optimization	
dihedral	single-point	ACN	THF	single-point	ACN	THF
ϕ	45.0°	45.3°	45.4°	−45.0°	−44.9°	−44.8°
δ_1	−146.3°	−149.6°	−148.5°	−151.1°	−147.0°	−147.4°
δ_2	117.1°	120.9°	117.4°	136.8°	139.0°	140.7°
δ_3	157.5°	157.7°	157.3°	60.9°	62.0°	61.2°
δ_4	−62.1°	−61.4°	−61.6°	−157.2°	−158.3°	−157.1°
δ_5	−78.4°	−79.1°	−78.9°	69.3°	70.4°	69.9°
δ_6	−68.2°	−68.5°	−68.9°	78.1°	79.3°	78.5°
ΔE (kJ/mol)		∼0	∼0		−1.0	−2.2

[a] The values of some relevant dihedral angles are reported as computed in the single-point calculation (second and fifth column) and after complete optimization in the two solvents (third, fourth, sixth, and seventh column). The single-point PCM calculation has been performed on the geometry obtained from a vacuum optimization of all BADBP internal coordinates but ϕ. In the last row, the energy difference between single-point and optimized geometry is reported, for ACN and THF, respectively.

4. Conclusions

The torsional energy profile for the rotation around the ring−ring bond of the BP group linked to a cholestanic backbone has been studied with DFT methods in the gas and condensed phases, using the CPCM approach in the latter case.

For the isolated molecule, the energy profile shows two symmetric minima at angles $\phi = \pm 45°$, with a barrier of ~40 kJ/mol at $\phi = 0°$. The barrier is lowered, and the symmetry is removed in the condensed phase, but the lower well turns out to be that at $\phi = +45°$, irrespective of the solvent.

This is in marked contrast with the experimental findings that indicate a favored M conformer when the phosphite is dissolved in ACN, whereas the lower minimum in THF belongs to the P diastereoisomer. This failure seems to indicate that the solvent effect on the torsional motion of the BP is related to local, specific interactions that are beyond the scope of any continuum description of the solvent, whose identity is mainly determined by the dielectric permittivity.

Support for this hypothesis comes from the aforementioned experimental evidence resulting from the CD spectra[8] of the compounds obtained when the BP unit is linked to position seven or three of the cholic acid. In particular, the latter finding points to an even distribution of diastereoisomers when the solvent can freely approach the BP. Taken together, the above observations outline a picture whereby a dominant screw sense is the result of a subtle balance of intra- and intermolecular interactions. In particular, the almost rigid cholestanic backbone might create different local environments through excluded volume effects, depending on the position where the BP unit is linked. These environments might act as a sort of molecular sieve, selecting solvent molecules according to their size and direction of approach.

Excluded volume effects are accounted for in the PCM description of the system through the shape and size of the cavity that contains the solute molecule. This is a delicate issue when implementing PCM calculations, and different approaches have been proposed.[17] We have tested the effect of the cavity description on the results by running a few calculations, again in the SES approach, but with no added spheres. The difference with the results shown in Figure 8, obtained by adding spheres to the cavity to smooth the surface, are minor and do not show a better agreement with the experimental data.

As a consequence, future investigations could be pursued along two different routes. The first would require supplementing the PCM description with a few explicit solvent molecules, whose position and orientations should be optimized. Because this choice appears to be quite demanding from a computational point of view, we plan to adopt a molecular dynamics simulation approach. This technique is capable of providing a reliable description of the solute plus discrete solvent system if an accurate force field for all relevant interactions is available. The intramolecular part of this force field will be obtained from ab initio calculations via the JOYCE program,[20,21] already tested on some mesogens with satisfactory results.[22,23] Both THF[24] and ACN[25] have been studied in the liquid phase with a few models, so solvent−solvent force fields are also readily available. Finally, because between the two phosphite conformers ($\phi = \pm 45°$) there is a barrier of tens of kilojoules per mole, a reliable sampling of the relevant potential energy surface can be achieved only with techniques explicitly devised to cope with rare events, for example, constrained dynamics or umbrella sampling.

References and Notes

(1) Balzani, V.; Venturi, M.; Credi, A. *Topics in Current Chemistry*; Kelly, T. R., Ed.; Springer: Berlin, 2005; Vol. 262.
(2) Zhao, Y. L.; Aprahamian, I.; Trabolsi, A.; Erina, N.; Stoddart, J. F. *J. Am. Chem. Soc.* **2008**, *130*, 6348.
(3) Saha, S.; Stoddart, J. F. *Chem. Soc. Rev.* **2007**, *36*, 77.
(4) Mirfakhrai, T.; Madden, J. D. W.; Baughman, R. H. *Mater. Today* **2007**, *10*, 30.
(5) Feringa, B. L.; Jager, W. F.; De Lange, B. *Tetrahedron* **1993**, *49*, 8267.
(6) Clayden, J.; Mitjans, D.; Youssef, L. H. *J. Am. Chem. Soc.* **2002**, *124*, 5266.
(7) Clayden, J.; Fletcher, S. P.; Rowbottom, S. J. M.; Helliwell, M. *Org. Lett.* **2009**, *11*, 2313.
(8) Iuliano, A.; Facchetti, S.; Uccello-Barretta, G. *J. Org. Chem.* **2006**, *71*, 4943.
(9) Diedrich, C.; Grimme, S. *J. Phys. Chem. A* **2003**, *107*, 2524.
(10) Frisch, M. J.; Trucks, G. W.; Schlegel, H. B.; Scuseria, G. E.; Robb, M. A.; Cheeseman, J. R.; Montgomery, J. A., Jr.; Vreven, T.; Kudin, K. N.; Burant, J. C.; Millam, J. M.; Iyengar, S. S.; Tomasi, J.; Barone, V.; Mennucci, B.; Cossi, M.; Scalmani, G.; Rega, N.; Petersson, G. A.; Nakatsuji, H.; Hada, M.; Ehara, M.; Toyota, K.; Fukuda, R.; Hasegawa, J.; Ishida, M.; Nakajima, T.; Honda, Y.; Kitao, O.; Nakai, H.; Klene, M.; Li, X.; Knox, J. E.; Hratchian, H. P.; Cross, J. B.; Bakken, V.; Adamo, C.; Jaramillo, J.; Gomperts, R.; Stratmann, R. E.; Yazyev, O.; Austin, A. J.; Cammi, R.; Pomelli, C.; Ochterski, J. W.; Ayala, P. Y.; Morokuma, K.; Voth, G. A.; Salvador, P.; Dannenberg, J. J.; Zakrzewski, V. G.; Dapprich, S.; Daniels, A. D.; Strain, M. C.; Farkas, O.; Malick, D. K.; Rabuck, A. D.; Raghavachari, K.; Foresman, J. B.; Ortiz, J. V.; Cui, Q.; Baboul, A. G.; Clifford, S.; Cioslowski, J.; Stefanov, B. B.; Liu, G.; Liashenko, A.; Piskorz, P.; Komaromi, I.; Martin, R. L.; Fox, D. J.; Keith, T.; Al-Laham, M. A.; Peng, C. Y.; Nanayakkara, A.; Challacombe, M.; Gill, P. M. W.; Johnson, B.; Chen, W.; Wong, M. W.; Gonzalez, C.; Pople, J. A.; *Gaussian 03*, revision C.02; Gaussian, Inc.: Wallingford, CT, 2004.
(11) Becke, A. D. *J. Chem. Phys.* **1993**, *98*, 5648.
(12) Tomasi, J.; Mennucci, B.; Cammi, R. *Chem. Rev* **2005**, *105*, 2999.
(13) Barone, V.; Cossi, M. *J. Phys. Chem. A* **1998**, *102*, 1995.
(14) Cossi, M.; Rega, N.; Scalmani, G.; Barone, V. *J. Comput. Chem.* **2003**, *24*, 669.
(15) Tsuzuki, S.; Tanabe, K. *J. Phys. Chem.* **1991**, *95*, 139.
(16) Clark, S. J.; Adam, C. J.; Cleaver, D. J.; Crain, J. *Liq. Cryst.* **1997**, *22*, 477.
(17) Tomasi, J.; Mennucci, B.; Cammi, R. *Chem. Rev* **2005**, *105*, 2999.
(18) Goller, A.; Grummt, U. *Chem. Phys. Lett.* **2000**, *321*, 399.
(19) Cacelli, I.; Prampolini, G. *J. Phys. Chem. A* **2003**, *107*, 8665.
(20) Cacelli, I.; Prampolini, G. *J. Chem. Theory Comput.* **2007**, *3*, 1803.
(21) Cacelli, I.; Prampolini, G. *JOYCE*: free software available under the terms of the GNU License; Pisa, Italy, 2007. http://tglc.dcci.unipi.it/.
(22) Cacelli, I.; Lami, C.; Prampolini, G. *J. Comput. Chem.* **2009**, *30*, 366.
(23) Cacelli, I.; Cimoli, A.; De Gaetani, L.; Prampolini, G.; Tani, A. *J. Chem. Theory Comput.* **2009**, *5*, 1865.
(24) Chandrasekhar, J.; Jorgensen, W. L. *J. Chem. Phys.* **1982**, *77*, 5073.
(25) Edwards, D.; Madden, P.; McDonald, I. *Mol. Phys.* **1984**, *51*, 1141.

JP905062Q